

Analyzing dexterous hands using a parallel robots framework

Júlia Borràs · Aaron M. Dollar

Received: 7 April 2013 / Accepted: 18 November 2013 / Published online: 30 November 2013
© Springer Science+Business Media New York 2013

Abstract Dexterous, within-hand manipulation, in which an object held in the fingertips is manipulated by the fingers, shares many similarities with parallel robots. However, their mathematical formulations appear to be substantially different. This paper introduces a formulation typical from parallel manipulators to model the kinetostatics of a hand-plus-object system, including the fingertip forces formulation to describe a feasible grasp. The framework also includes compliance in the joint and considers pulling cable transmission mechanisms to model underactuated hands. The resultant static equilibrium equations are equivalent to the typical grasping formulation, but the involved matrices are different, allowing the interpretation of the resulting Jacobian matrix in terms of wrenches exerted by the joints. We primarily focus our efforts on describing in detail the theoretical framework, and follow this with an example application using a three-fingered underactuated hand. We show how the natural redundancy present in fully-actuated hands can be eliminated using underactuation, leading to simplified non-redundant systems that are easier to control. For the studied hand, we show how to use the framework to analyze the design parameters involved in the underactuation and their relationship with the resultant feasible workspace where the object can be manipulated.

Keywords Multifingered hands · Screw theory · Parallel manipulators

J. Borràs (✉) · A. M. Dollar
Department of Mechanical Engineering and Materials Science,
Yale University, New Haven, CT, USA
e-mail: julia.borrassol@yale.edu

A. M. Dollar
e-mail: aaron.dollar@yale.edu

1 Introduction

Analyzing dexterous manipulation with multi-fingered hands is challenging, in part due to the difficulties in dealing with the closed-loop kinematic chain established between the fingers and object and the resulting potential for an overconstrained system. This paper revisits a mathematical framework typically used with parallel platforms for the study of robotic hands performing dexterous, within-hand manipulations that have a kinematic structure equivalent to a parallel manipulator (Fig. 1)

Earlier work has acknowledged the equivalence of the hand-plus-object as a closed kinematic chain (Kerr and Roth 1986; Montana 1995), but generally used mathematical frameworks from open serial chains (Murray et al. 1994; Prattichizzo and Trinkle 2008). Most of the dimensional synthesis of robotic hands has been done studying the properties of the independent fingers (e.g. Salisbury and Craig 1982). Other degeneracies due to the cooperation of the fingers with the object are commonly used only to quantify the quality of a particular grasp (Bicchi et al. 1995; Shimoga 1996) and not to analyze the whole hand.

The framework proposed here models the system of hand-plus-object as a whole. This is useful to analyze the size of the manipulation workspace and to study other important properties, such as singularities within the workspace, that in practice can reduce the size of the usable workspace (Hubert and Merlet 2009). Robotic hands can benefit from the literature of parallel robots in several aspects. For instance, singularities have been widely studied (Zlatanov 1998) and manipulability indexes have been proven to be not very good indicators of the quality of the manipulability through the workspace (Merlet 2006a), concepts that can be directly translated to robotic hands manipulating objects. Transfer of knowledge



Fig. 1 When an open hand is closed to grasp an object, the kinematic structure is equivalent to a parallel robot

between these fields is starting to be explored in [Ebert-Uphoff and Voglewede \(2004\)](#).

In this paper, we propose a formulation to analyze multi-fingered hands manipulating rigid objects within a precision fingertip grasp, using a point contact with friction, or hard-finger model ([Kerr and Roth 1986](#); [Prattichizzo and Trinkle 2008](#)). We show that the proposed parallel robots framework can be applied to study the static properties of a hand holding an object, provided that we restrict the analysis only to those configurations of the workspace for which the fingertip forces are within their respective friction cones. The proposed framework uses theory of reciprocal screws, which has been applied to hands during the early 90s, at the origin on hand kinematic analysis ([Hunt et al. 1991](#); [Romdhane and Duffy 1990](#)) but only in few recent works, like the project on the Metamorphic Multifingered hand from [Cui and Dai \(2012\)](#) and [Dai et al. \(2009\)](#).

A secondary aim of this paper is to consider modeling *underactuated* hands for the study of their dexterous manipulation workspace. Typical parallel robots use only as many joint actuators as degrees of freedom (DoF) the platform has to move. Even though each leg itself has usually as many DoFs as platform DoFs, only one or two of the joints per leg are actuated, called active joints, and the rest are left free to move through passive joints. Having an exactly constrained system simplifies the control of the resulting mechanism, as the free moving joints automatically adapt to hold the kinematic constraints.

On the contrary, robotic hands need to have all of the joints of the fingers actuated, to be able to be articulated and avoid collapsing under their own weight before contact with an object. After contact with an object is made on the distal links of the fingers, the equivalent mechanism is a parallel platform where all the joints are generally actuated except for the platform attachments (i.e. finger contacts). This typically results in a redundantly actuated parallel configuration ([Müller 2008](#)). Adding one or two degrees of redundancy is sometimes used in parallel manipulators to reduce singularities and to increase the usable workspace ([Dasgupta and Mruthyunjaya 1998](#)). However, highly redundant configurations have substantial drawbacks typical of overly constrained systems, such as errors due to internal forces that complicate the calibration and a complex control process.

This issue can be mitigated using differential transmissions implemented to produce underactuated fingers. Underactuated hands typically use one actuator to control two or more joints, so that all the joints are active but are coupled together through some sort of differential mechanism ([Birglen and Laliberte 2008](#)). The coupling can be implemented through cables and pulleys or linkages ([Balasubramanian et al. 2012](#); [Birglen and Laliberte 2008](#); [Dollar and Howe 2010](#); [Hirose and Umeteni 1978](#)), and generally require one or more compliant elements to provide a loose constraint on the unconstrained DoFs and/or provide a means of antagonistic actuation to the tendon. In particular, when the transmission is implemented with pulling cables, underactuation can be easily integrated in the proposed framework.

This work focuses on the static analysis of hands holding objects in a precision grasp, analyzing the conditions under which a grasp is feasible and therefore belongs to the manipulable workspace of the hand/object system. The framework can be used to model fully actuated hands and also underactuated hands. As an example, we apply it to an underactuated hand with three fingers and two links per finger. For this architecture, we study how the underactuation design parameters such as the transmission ratio and the stiffness constants of the finger joints can modify the size of the feasible workspace. This paper is an extension of a conference paper by the authors ([Borràs and Dollar 2013b](#)), expanded to include a detailed exposition of the methodology to obtain the model equations and to complete the design parameter analysis of a 3-URS hand using the framework.

In Sect. 2 we start introducing the mathematical framework that is commonly used in the parallel robots literature ([Merlet 2006b](#); [Tsai 1999](#)), adapting it to the analysis of an underactuated robotic hand and defining how the friction cone conditions are applied under the new framework. In Sect. 3 we show an example of how to apply the framework and we study the different workspace sizes depending on the design parameters. Finally, Sect. 4 gives some conclusions, and points out future studies using the proposed framework.

2 Mathematical model of the hand-plus-object

The literature of robotic hands commonly models the hand as a set of serial chains (the fingers) that have to collaborate to manipulate an object. The grasp matrix \mathbf{G} is normally built from the change of coordinates matrix from a reference frame fixed at the center of mass of the object to a local reference frame located at each contact point. The hand Jacobian \mathbf{J}_h is obtained by stacking in diagonal the Jacobian matrices of the serial chains of each finger. The contact model consists of a matrix \mathbf{H} that will select the appropriate coordinates and the static equilibrium equations are solved by imposing the coincidence between the contact points and the fingertips (Bicchi et al. 1995; Prattichizzo and Trinkle 2008).

Here, we present an alternative approach to define the matrices that relate the joint velocities/torques with the resultant object twist/wrench using a framework that is widely used in the context of parallel manipulators. Indeed, a hand manipulating an object is equivalent to a parallel manipulator, with the additional constraint that the contact force at each fingertip must be within the friction cone. The resultant mathematical systems are equivalent to the system solved in classic grasping notation such as (Shimoga 1996), but the actual matrices are different (Borràs and Dollar 2013a). Furthermore, the geometrical interpretations used in parallel manipulators can give new insights in several aspects of the dexterous hands, such as workspace optimization, hand design, and others.

Depending on the contact model, the corresponding equivalent parallel manipulator will change. The hard finger or point contact with friction transmits only the direction of the force from the finger to the object. Thus, it is kinematically equivalent to a spherical joint. The soft finger, where the fingers can transmit not only the force but also the moment of the force around the normal component at the fingertip, is equivalent to a parallel manipulator that uses universal joints in its platform attachments. In this work, we will consider the first model, but a similar analysis can be done with the second. The rolling contact model is more complex and its integration with the framework is left for future work.

Consider the hand-plus-object system formed by the hand, the contact points and the object. The object can be moved in a maximum of 6 DoF, three for position and three for orientations, defined in a 6-dim vector \mathbf{x} . However, depending on the number of fingers, links, and joints, the object can be manipulated in only n DoF, where n is the mobility of the system. The mobility can be computed using the Grübler–Kutzbach criterion (Downing et al. 2002; Mason and Salisbury 1985). If $n < 6$, the system is called lower mobility (Kanaan et al. 2009), that is, the workspace where the object can be manipulated with the fingers is a n dimensional subspace of the 6-dim task space. If the mobility is higher than 6, the object

workspace is still 6 dimensional, but it has kinematic redundancy (Mohamed and Gosselin 2005).

For simplicity, we consider all the joints 1 DoF. In other words, a universal (spherical) joint is considered as two (three) rotational joints with intersecting axes. In a generic hand with l fingers with m_i joints each, the total number of joints of the hand is $m = \sum_{i=1}^l m_i$. The total number of joints of the hand-and-object system is $m + 3l$, that is, the hand joints plus the platform attachment joints, which are considered free to move (passive). Let

$$\Theta = (\theta_1, \dots, \theta_m)^T \quad (1)$$

be the vector of all the hand joint angles. Only n of them are independent and determine the position of the object. Generally, all joints are actuated and thus, the number of motors is $n_a = m > n$. In the context of parallel manipulators, this is known as a redundantly actuated system. If the hand uses underactuation, the number of motors can be lower. If $n_a = n$, that is, we have as many motors as mobility, we say that the hand-plus-object system is fully-actuated. Note that we need at least n motors to be able to control all the mobility DoFs of the object. If less motors are used, there will be $n - n_a$ uncontrolled DoFs. This is used in some underactuated hands as a desired passive compliant DoF.

Any value of Θ determines a configuration of the hand, but when manipulating the object, the only feasible configurations are those that satisfy the *kinematic constraints*, namely, a set of equations that can be written as $H(\Theta) = 0$. These are normally distance constraints between the fingertips, that must remain constant, assuming that the object is rigid enough and that the hand does not re-grasp the object. To consider soft objects, the constraints should be considered as inequalities.

We define the kinematic configuration space of the hand holding the object as

$$C = \{\Theta \in \mathbb{R}^m | H(\Theta) = 0\} \quad (2)$$

The position and orientation of the object are defined by an element of $SE(3)$, in our case, a position vector \mathbf{p} and a rotation matrix \mathbf{R} . For any feasible configuration, we can compute the position and orientation of the object by solving the loop equations, which can be defined by requiring the fingertip coordinates and the object contact coordinates to be coincident. We can write the solution of the loop equation as the map $FK : C \rightarrow SE(3)$, usually known as forward kinematic problem. The kinematic workspace of the manipulated object is then defined as

$$WS = \{FK(\Theta) | \Theta \in C\} \subset SE(3) \quad (3)$$

The resolution of the inverse kinematics consist in, given the position and orientation of the object, find the location of the contact points and then solve the inverse kinematic of each of the fingers. Note that if the finger has more than three joints,

there can be a set of solutions of dimension $(m_i - 3)$. In this case, a single solution is usually chosen optimizing a certain objective function (Shimoga 1996).

There are several approaches to define the matrix that maps the joint velocities (or joint torques) to the platform/object twist (or wrench). Here we will use the theory of reciprocal screws to define this matrix, following Chapter 5.6 in Tsai (1999), or Merlet (2006b) and Mohamed and Duffy (1985).

The twist induced by a rotational joint located at the position vector \mathbf{p} , with an axis of rotation in direction \mathbf{s} is

$$\mathcal{S}_r = (\mathbf{p} \times \mathbf{s}, \mathbf{s})^T,$$

while a twist induced by a prismatic joint along an axis \mathbf{s} is $\mathcal{S}_p = (\mathbf{s}, 0)^T$.

Following Tsai (1999) and Mohamed and Duffy (1985), the twist transmitted to the platform/object, $\mathbf{T} = (\mathbf{v}, \Omega)$, can be written as the sum of all the twists induced by the prismatic or rotational joints of each leg (including the passive ones). If we consider the hard finger contact model, each finger has three extra passive joints corresponding to the contact point (modeled as a spherical joint):

$$\mathbf{T} = \sum_{j=1}^{m_i+3} \dot{\theta}_{ij} \mathcal{S}_i j, \quad i = 1, \dots, l \tag{4}$$

We want to eliminate from the above system the velocities of the passive joints. To this end, we multiply both sides of this equation by the set of screws that are reciprocal to all the passive joints. Two screws $\mathcal{S}_1 = (p_1 \times s_1, s_1)^T$ and $\mathcal{S}_2 = (p_2 \times s_2, s_2)^T$ are reciprocal when their reciprocal product is zero, that is

$$\mathcal{S}_1 * \mathcal{S}_2 = \mathcal{S}_1^T \Delta \mathcal{S}_2 = (p_1 \times s_1) \cdot s_2 + (p_2 \times s_2) \cdot s_1 = 0,$$

where $\Delta = \begin{pmatrix} 0 & I_3 \\ I_3 & 0 \end{pmatrix}$.

Historically, this step has been done with a lot of mechanical intuition, but lately more systematic methods have been proposed (Zhao et al. 2009). All joints in the fingers are actuated, and the contacts are free to move. Thus, we have to define a system of screws reciprocal to the three passive joints corresponding to the contact point. As a system of three screws through a point is self-reciprocal (Dai and Jones 2001; Gibson and Hunt 1990) we can chose any system of three screws through the contact point to define the reciprocal system. The resultant matrix will be independent of this choice.

Let us call $\mathcal{S}_{ri} = (\mathcal{S}_{rik})$ for $k = 1, \dots, 3$ the reciprocal system to the passive joints of leg i . If we apply the reciprocal product at both sides of Eq. (4), all the screws associated with passive joints at the right side vanish, leading to

$$\mathcal{S}_{ri}^T \Delta \mathbf{T} = (\mathcal{S}_{rik}^T \Delta \mathcal{S}_{ij}) \begin{pmatrix} \dot{\theta}_i 1 \\ \vdots \\ \dot{\theta}_{im_i} \end{pmatrix}, \quad i = 1, \dots, l \tag{5}$$

where the matrices $\mathbf{J}_{pi} = \mathcal{S}_{ri}^T \Delta$ contain in each row the screws reciprocal to the passive joints of leg i , and thus, they are 3×6 matrices and $\mathbf{J}_{\Theta i} = (\mathcal{S}_{rik}^T \Delta \mathcal{S}_{ij})$ contains the reciprocal products of the reciprocal screws with the finger joint screws, and thus, they are $3 \times m_i$. We can rewrite this system in a single matrix form leading to

$$\mathbf{J}_p \mathbf{T} = \mathbf{J}_{\Theta} \dot{\Theta}, \tag{6}$$

where \mathbf{J}_p is a $3l \times 6$ matrix and \mathbf{J}_{Θ} a $3l \times m$ with expressions

$$\mathbf{J}_p = \begin{pmatrix} \mathbf{J}_{p1} \\ \vdots \\ \mathbf{J}_{pl} \end{pmatrix} \text{ and } \mathbf{J}_{\Theta} = \begin{pmatrix} \mathbf{J}_{\Theta 1} & 0 & 0 \\ 0 & \ddots & 0 \\ 0 & 0 & \mathbf{J}_{\Theta l} \end{pmatrix}. \tag{7}$$

For a hand with three fingers and three joints per finger, we have shown in Borràs and Dollar (2013a) that these two matrices can be multiplied as $\mathbf{J} = \mathbf{J}_{\Theta}^{-1} \mathbf{J}_p$ and the resultant Jacobian matrix is equivalent to the hand Jacobian plus grasp matrix system in Prattichizzo and Trinkle (2008). In general, the matrix \mathbf{J}_{Θ} is not square, but we can use the left pseudo-inverse of the tall matrix \mathbf{J}_p to write $\mathbf{J}_p^+ \mathbf{J}_{\Theta} \dot{\Theta} = \mathbf{T}$.

We can write the static equilibrium equations substituting these expressions in the principle of virtual work (Tsai 1999) leading to

$$-\mathbf{W} = \mathbf{J}_p^T \mathbf{J}_{\Theta}^{+T} \boldsymbol{\tau} \tag{8}$$

where $\boldsymbol{\tau} = (\tau_i)$, for $i = 1, \dots, m$, is the vector of torques done by each joint i , \mathbf{W} is the total external wrench applied on the object, and \mathbf{J}_{Θ}^{+T} is the left pseudo inverse of the transposed matrix \mathbf{J}_{Θ} . The matrix

$$\mathbf{J}^T = \mathbf{J}_p^T \mathbf{J}_{\Theta}^{+T} \tag{9}$$

is $6 \times m$ and it can be interpreted in terms of the geometry of the mechanism; this fact has been applied in the parallel robot literature for easier detection of singularities and as a tool for optimal design (Merlet 2006b).

This system models the hand statics, provided that we discard those configurations for which the resulting fingertip forces are outside the friction cone, as it will be detailed in Sect. 2.2.

Equation (8) defines the static equilibrium of the hand-plus-object. When a configuration is in static equilibrium for any direction of \mathbf{W} , then the hand-plus-object is called force closure grasp (Prattichizzo and Trinkle 2008).

Finally, we also want to consider compliance in parallel with the joint actuators. Each torque τ_i will be composed of two components, one from the actuation torque and one from the spring torque, obtained using the Hooke's law. This is

$$\tau_i = {}^a \tau_i - K_i (\theta_i - \delta_i), \tag{10}$$

where $K_i > 0$ is the spring stiffness constant and δ_i is the rest configuration angles for the fingers. We are assuming that all joints are rotational joints, so that θ_i are angles and the springs are torsional springs, but the same can be done with prismatic actuators and linear springs (Borràs and Dollar 2012).

For a given configuration and a given external applied force, the system in (8) is a linear system where the unknowns are the m actuation torques

$$-W = J^{T^a} \tau + J^{T^c} \tau, \quad (11)$$

where we have split the torque vector into the actuation torques ${}^a\tau = ({}^a\tau_i)$ and the compliant torques ${}^c\tau = (-K_i(\theta_i - \delta_i))$.

As there are fewer equations than unknowns, there is a $(m - 6)$ -dimensional set of solutions for each configuration. A single solution can be chosen optimizing, for instance, the maximum actuation torque to be as small as possible, constrained by imposing the resulting fingertip forces to be inside the friction cones.

The Jacobian matrix in (9) characterizes the singularities of the system, as those configurations for which the matrix loses rank. Classic hands papers consider singularities only of the finger serial chains (Salisbury and Craig 1982). In the parallel robots literature, these kind of singularities are classified as type I (or serial) singularities in the Gosselin and Angeles (1990) classification or Redundant Input in Zlatanov (1998). They occur when the matrix J_{\ominus} loses rank. These singularities result in a loss of DoF, in other words, only some forces can be transmitted to the object. Typically, it is more challenging to detect the second type of singularities, called type II, parallel or Redundant Output singularities, which occur when the matrix J_p loses rank. Under this type of singularity the manipulator gains uncontrollable DoF. For parallel manipulators, one of the consequences of this kind of singularities is that in the neighborhood of a singularity, small applied forces may result in very big actuation torques which may lead to the breakdown of the robot. In the case of hands, it results in the loss of the object or in the breaking of the object under the pressure of the fingers. In both cases, singularities define limits of the usable workspace (Gosselin and Angeles 1990; Hubert and Merlet 2004).

2.1 Underactuated hands

Underactuated hands have become very popular due to its adaptation to unstructured environments. When using underactuated fingers, some of the motors control two or more of the joints. Depending on the transmission mechanism, extra Jacobian matrices have to be added to the above equations (Birglen and Laliberte 2008). But when using pulling cables, we can model the transmission mechanism as a coupling

between the torques exerted by the joints actuated by the same motor. Such coupling depends only on the ratio between the radii of the rotational joints, that will be called the transmission ratio r (Balasubramanian et al. 2012).

Let us assume that we introduce as many couplings as necessary to have only n actuators, meaning that the resulting system is no longer redundant. This means that some of the torques will be related to others through a transmission ratio r_k , that is, ${}^a\tau_k = r_k {}^a\tau_i$ for $k = 1, \dots, m - n$ of the actuated torques.

Then, we can rewrite Eq. (11) as

$$-W = J_a^{T^a} \tilde{\tau} + J^{T^c} \tau \quad (12)$$

where ${}^a\tilde{\tau}$ is an n -dimensional vector that contains only the independent actuation torques. The matrix $J_a^{T^a}$ is a square matrix that can be obtained from J^T using linear combinations of the columns with the scaling factors r_k . See Sect. 3 for an example.

Note that the underactuation is modeled with a spring and a cable in parallel, but the spring acts in parallel with the motor only when the cable is pulling, and as a passive compliant joint otherwise. To take that into account without introducing too much complexity to the system, we simply solve the system considering the springs in parallel with the motors, and we discard any configuration where the actuation torque is not of the opposite sign of the spring torque. In other words, depending on the routing of the cable, we discard positive or negative actuation torques.

For a given configuration, the above system is a square linear system. In this case, there is a one to one correspondence between the external applied force and the corresponding actuation torques.

It is also important to notice that a new singularity appears, because when $\det(J_a^{T^a}) = 0$ the above system is singular. By construction, close to a singularity where $J_a^{T^a}$ loses rank, small applied forces can lead to very big actuation torques, and thus, this matrix defines the limit of the static workspace (Hubert and Merlet 2009).

This means that an underactuated hand will have, in general, a smaller workspace, as more configurations will be close to singularities. However, with improved design processes, the workspace can be large enough for the required tasks. Thus, underactuation is a promising feature for the design of hands with more efficient manipulation processes, in contrast to fully actuated hands, as the forward static problem is much simpler, resulting in simpler dynamics and control processes.

In Sect. 3.3 we will study how the spring free lengths, stiffness constants and the transmission ratio play an important role in the maximization of the size of the usable workspace.

2.2 Fingertip forces and friction cone conditions.

We have already mentioned that the parallel robots mathematical framework can be applied to hands as long as the fingertip forces are constrained to be inside the friction cones. In this section we describe how we can write such conditions in a natural way using our framework.

Recall the hand with l fingers with m_i joints each (so, $m = \sum_{i=1}^l m_i$). From Eq. (9), consider the columns of the Jacobian matrix as $\mathbf{J}^T = (s_{ij})$ for $i = 1, \dots, l$ and $j = 1, \dots, m_i$. Each column has the form $s_{ij} = (\mathbf{f}_{ij}, \mathbf{m}_{ij})^T$, where \mathbf{f}_{ij} corresponds to the force the joint j transmits to the fingertip of the finger i , with magnitude τ_{ij} , and \mathbf{m}_{ij} its corresponding moment.

Then, we can write the wrenches at the fingertips as

$$\mathbf{W}_i = (s_{i1}, \dots, s_{im_i}) \begin{pmatrix} \tau_{i1} \\ \vdots \\ \tau_{im_i} \end{pmatrix}, \quad \text{for } i = 1, \dots, l. \quad (13)$$

In other words, the fingertip wrench can be written as $\mathbf{W}_i = (\mathbf{F}_i, \mathbf{M}_i)$, where the fingertip force will be given by $\mathbf{F}_i = \tau_{i1}\mathbf{f}_{i1} + \dots + \tau_{im_i}\mathbf{f}_{im_i}$ (see Fig. 3 for an example). The other three components correspond to the moment done by \mathbf{F}_i , $\mathbf{M}_i = \mathbf{c}_i \times \mathbf{F}_i$. The sum of all the fingertip forces and moments is the resulting output force and moment on the object¹.

In Prattichizzo and Trinkle (2008) the friction cone is defined with respect to the coordinate frame attached to the contact point, whose axes are defined as $R_i = \{\mathbf{n}_i, \mathbf{t}_i, \mathbf{o}_i\}$, where \mathbf{n}_i is the unit vector directed from the contact point to the center of the object, and the other two are defined orthogonal unit vectors. While in the Prattichizzo and Trinkle work these vectors are used to define the Jacobian matrices, in the presented framework we just need the definition of \mathbf{n}_i to project the fingertip force. Assuming a spherical object, we can define the vector as $\mathbf{n}_i = \mathbf{p} - \mathbf{c}_i$, \mathbf{p} being the position vector of the object and \mathbf{c}_i the contact point. Then, we split the fingertip force \mathbf{F}_i into the projection on \mathbf{n}_i , given by ${}^n F_i = \mathbf{n}_i^T \mathbf{F}_i$, and the projection on the normal plane to the vector, ${}^\perp F_i = \|(\mathbf{I}d - \mathbf{n}_i \mathbf{n}_i^T) \mathbf{F}_i\|$. The fingertip is inside the friction cone as long as

$${}^\perp F_i \leq \mu^n F_i, \quad (14)$$

where μ represents the amplitude of the friction cone which will be assumed to be 0.7 for the simulations in Sect. 3.

At a given configuration, the expression of the fingertip forces depends only on the torques of the joints at each finger, which depend on the actuation torques and on the spring parameters. If the force is outside the friction cone, the configuration is considered out of the feasible workspace.

¹ All the coordinates are with respect to the palm reference frame.

2.3 On the hard-finger contact model

In the previous section we have studied the mathematical model of the hand-plus-object system using the hard-finger contact model, equivalent to a spherical joint.

Even though such model may be not entirely realistic of the behavior of a hand, it does introduce several advantages to study the mobility and shape of the workspace. In the context of parallel robots it is known that the Jacobian matrix of parallel robots that use spherical joints as platform attachment will always involve the Plücker coordinates of a line associated to the link connecting the leg to the end effector (see Chapter 5.2.3 in Merlet 2006b book). That means that the columns of the final matrix \mathbf{J}^T can always be interpreted in terms of wrenches.

In addition, because the twist system associated to a spherical joint is self-reciprocal, any three screws through the contact point can be chosen to define the system of reciprocal screws. In Borràs and Dollar (2013a) it was pointed out how the choice of that system shapes the structure of the matrices \mathbf{J}_p and \mathbf{J}_\ominus without altering the shape of \mathbf{J}^T , and thus, convenient choices can be done for different purposes. For instance, in Cui and Dai (2012) they chose the reciprocal system to facilitate the singular value decomposition of the finger Jacobian. In the context of parallel robots, the reciprocal system is chosen to make the matrix \mathbf{J}_\ominus as diagonal as possible to facilitate its inversion and the geometrical interpretation of \mathbf{J}^T .

3 Application example: a 3-URS hand

In this section we apply the formulation introduced in the previous section to a 3-URS hand (Fig. 1). This architecture is similar to several hands such as the Barrett hand (Townsend 2000) or the JPL hand (Salisbury and Craig 1982).

We assume the object is a disk with radius R_o and the contact points are uniformly distributed around it. The fixed reference frame is located at the center of the palm and the mobile frame centered at the center of mass of the object. Without loss of generality, we can write the coordinates of the palm attachments and the contact points with respect to the local reference frames as $\tilde{\mathbf{a}}_i$ and $\tilde{\mathbf{c}}_i$, respectively, with zero z coordinate (Fig. 2).

The position and orientation of the object with respect to the palm reference frame are given by a position vector $\mathbf{p} \in \mathbb{R}^3$ and a rotation matrix $\mathbf{R} \in SO(3)$. Then, the coordinates of the attachments with respect to the palm reference frame are $\mathbf{a}_i = \tilde{\mathbf{a}}_i$ and

$$\mathbf{c}_i = \mathbf{p} + \mathbf{R}\tilde{\mathbf{c}}_i. \quad (15)$$

As we assume contact, the coordinates of the contact points are the same as the coordinates of the fingertips, which

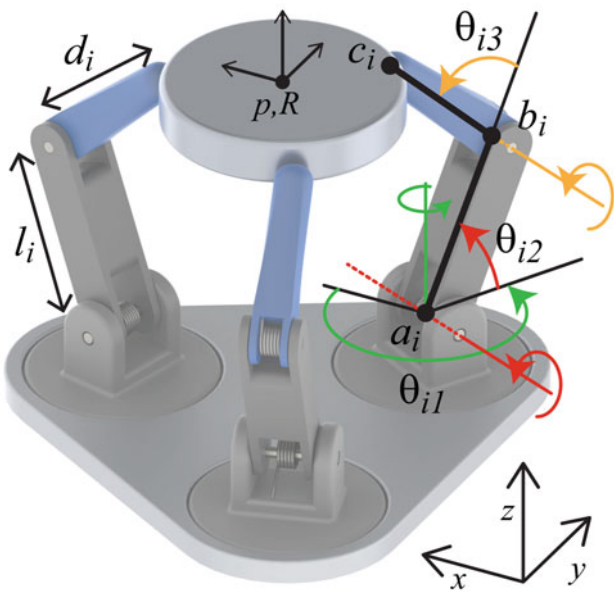


Fig. 2 Kinematic model of the studied hand. The center points of the base joints are equally distributed around a circumference of radius R_B , and the contact points around a circumference of radius R_o

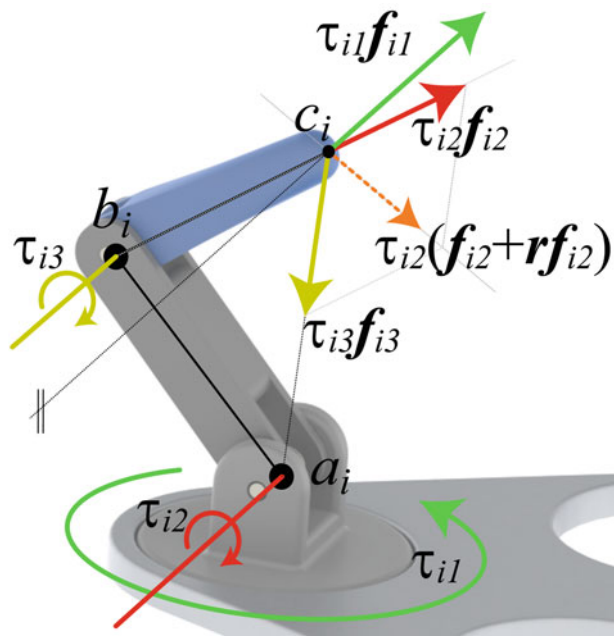


Fig. 3 Force transmitted to the fingertip under the torque exerted for each joint for the three actuated joints in each finger. The expression of the fingertip force is given by $\tau_{i1}f_{i1} + \tau_{i2}f_{i2} + \tau_{i3}f_{i3}$. For the under-actuated hand, the two forces f_{i2} and f_{i3} are merged depending on the transmission ratio r

can be parameterized following the steps in Chapter 2.2 of (Murray et al. 1994) as

$$c_i = a_i + h_i (0, 0, 1)^T + w_i (\cos(\theta_{i1}), \sin(\theta_{i1}), 0)^T, \tag{16}$$

where

$$\begin{aligned} h_i &= l_i \sin(\theta_{i2}) + d_i \sin(\theta_{i2} + \theta_{i3}), \\ w_i &= l_i \cos(\theta_{i2}) + d_i \cos(\theta_{i2} + \theta_{i3}), \end{aligned} \tag{17}$$

and l_i and d_i are the lengths of the proximal and distal links of the i th finger, respectively. We can obtain a similar parameterization of the distal joint centers (b_i in Fig. 2). Alternatively, a similar parameterization can be obtained using Denavit–Hartenberg parameters (Denavit and Hartenberg 1955).

The inverse and forward kinematics can be obtained by solving the system resulting from equating Eqs. (15) and (16). For these fingers, we can solve the forward kinematics function $FK(\Theta)$ and the inverse kinematics $IK(p, R)$ in a closed form solution. The kinematic constraints are given by the system $\{\|c_i - c_j\|^2 = 3R_o^2, i \neq j\}$.

Any set of three screws through the contact point can be used as the reciprocal system. However, in the context of parallel robots, it is convenient to choose each screw to be reciprocal to the passive joints plus two of the actuated. This may not always be possible, but in this case the system is fully determined leading to

$$\begin{aligned} \$_{ri1} &= (z_i, c_i \times z_i), \\ \$_{ri2} &= (c_i - b_i, c_i \times (c_i - b_i)) \\ \$_{ri3} &= (c_i - a_i, c_i \times (c_i - a_i)), \end{aligned} \tag{18}$$

where $z_i = (\sin(\theta_{i1}), -\cos(\theta_{i1}), 0)$ is the axis of rotation of the second and third joints of the finger i .

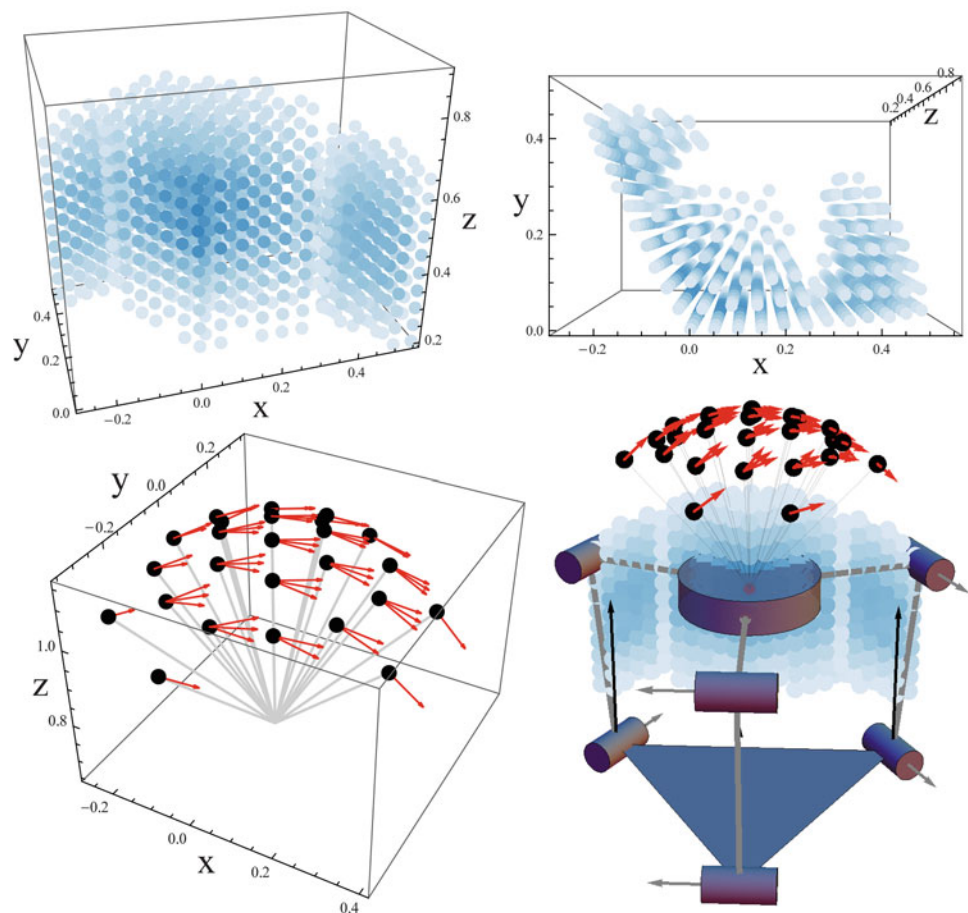
Using the above screws, J_Θ is a 9×9 diagonal matrix, and as a result we can write the Jacobian in Eq. (9) as the 6×9 matrix $J^T = (\dots s_{i1} s_{i2} s_{i3} \dots)$, for $i = 1, 2, 3$, where s_{ij} is the wrench corresponding to the action of the joint j of the finger i with expressions

$$\begin{aligned} s_{i1} &= \frac{-1}{w_i} \$_{ri1} \\ s_{i2} &= \frac{1}{l_i d_i \sin(\theta_{i3})} \$_{ri2} \\ s_{i3} &= \frac{-1}{l_i d_i \sin(\theta_{i3})} \$_{ri3} \end{aligned} \tag{19}$$

where w_i is defined in Eq. (17). See Fig. 3 for a graphical representation of those screws. This is the main difference from the usual framework used for hands. These three screws at each finger will define the fingertip wrench as $\tau_{i1}s_{i1} + \tau_{i2}s_{i2} + \tau_{i3}s_{i3}$. Choosing any other system of reciprocal screws leads to a non-diagonal matrix J_Θ , therefore, the resulting columns of J^T are linear combinations of the chosen reciprocal screws.

We consider a pulling cable that controls the 2nd and the 3rd joints, so that their corresponding torques are $\tau_{i2} = R_2 t$ and $\tau_{i3} = R_3 t$ where t is the tension of the cable and R_j are the radii of the pulleys located at the corresponding joints

Fig. 4 *Top* Two views of a third of the kinematic workspace. Each *dot* represents the position vector of the center of mass of the object, with *darker color* the more orientations it can reach from the position. *Bottom* Representation of the orientations at the position with maximum reachable orientations. Each *dot* on the sphere represents the direction of the vector normal to the plane formed by the three contact points, and the *arrow* the rotation around the axis *z*. *Bottom right figure* shows the workspaces with respect to the hand-plus-object



(equal for all fingers). For simplicity, we can write $\tau_{i3} = (R_3/R_2)\tau_{i2} = r\tau_{i2}$, where r will be called the transmission ratio (Balasubramanian et al. 2012). Then, J_a^T in Eq. (12) is a 6×6 matrix that can be obtained from J^T as

$$J_a^T = (\dots, s_{i1}, s_{i2} + rs_{i3}, \dots), \tag{20}$$

and the vector of actuation torques is ${}^a\tau = (\tau_{11}, \tau_{12}, \tau_{21}, \tau_{22}, \tau_{31}, \tau_{32})^T$. Note that the magnitude of the tension force exerted by the cable is given by $t = \frac{\tau_{i2}}{R_2}$.

All the simulations were run in Mathematica 9 (Wolfram Research Inc., Champaign, IL), for a hand with palm radius $R_B = 0.5$, an object of radius $R_o = 0.2$ and the dimensions of the finger links $l_i = 0.625$ and $d_i = 0.375$, for $i = 1, 2, 3$.

For simplicity, we omit units, but all magnitudes are in international units (m, N, Nm).

3.1 Kinematic workspace vs. feasible workspace

We obtain a representation of the kinematic workspace by sweeping the 6 dimensional space $SE(3)$ represented by the three translational parameters (p_x, p_y, p_z) and the three rotational parameters. Two of the rotational parameters are represented by points on a sphere that represent the orientation

of the vector normal to the plane formed by the three contact points. The last rotational parameter is the rotation around that normal vector, represented by the red arrow on top of the normal vector (Fig. 4 (bottom)). For each position and orientation, we solve the forward kinematics at each step, discarding any pose with non-real solution.

Representing a six dimensional space is difficult. In the workspace shown in Fig. 4, we paint each dot with a color code, darker when the object can reach more orientations. This workspace contains a total of 12,132 configurations, corresponding to a third of the position workspace (the other two thirds are symmetric with respect to the three legs) and half of the rotations around the z axis.

With the proposed underactuated hand, the system in Eq. (12) is square and thus, for each configuration, we state a one to one relationship between external force and actuation torque. While in a fully actuated hand this system is often redundant and the solution can be optimized to move the fingertip force inside the friction cone, in this case there is no possible optimization. However, preliminary results in Boràs and Dollar (2013b) show that the compliant joints acting in parallel with the cable play a significant role in the total size of the feasible workspace. Here we complete the study that

characterizes the relationship between the spring parameters, the transmission ratio and the size of the feasible workspace.

The underactuated joints are modeled as a motor acting in parallel with a spring (Eq. (11)), provided that the torque exerted by the springs and the torques exerted by the cables are of opposite signs. The torque exerted by the springs are ${}^c\tau_{i2} = K_2 (\theta_{i2} - \delta_2)$ and ${}^c\tau_{i3} = K_3 (\theta_{i3} - \delta_3)$, which depend on four parameters $\{K_2, K_3, \delta_2, \delta_3\}$. Note that the components corresponding to the first joints are ${}^c\tau_{i1} = 0$.

For each configuration, we solve the system in Eq. (12) for ${}^a\tau$, and then compute the corresponding fingertip forces. A configuration will be considered part of the feasible workspace if the fingertip forces are inside the friction cone and if the cables are only exerting positive torques. In other words, the springs act to open the hand and the cables act to close it. To set the springs to open the hands, we set the resting configurations to $\{\delta_2 = 0, \delta_3 = 0\}$. That mechanism is known in prosthetics as an active-close or voluntary-close device (Smit and Plettenburg 2010). Considering only negative torques would lead to an active-open device.

Note that each configuration of the feasible workspace is in static equilibrium for a given force. In other words, they do not represent force closure grasps. The feasible workspace will always be a subspace of the kinematic workspace. We will represent the sizes of the feasible workspaces as percentages of coverage of the kinematic workspace.

3.2 Overview of previous results

In a preliminary version of this work (Borràs and Dolár 2013b), we optimized independently two slices of the workspace, one corresponding to a fix position and the other corresponding to a fix orientation. The exploration of the parameter space show that bigger transmission ratios where

obtained when maximizing the workspace with a fix orientation that move the object in different positions. On the contrary, smaller transmission ratios maximized the workspace where the hand fixes the object in a position and varies the orientation.

In the next section, we consider the full workspace that combines both positions and orientations. In addition, we explore in detail the relationship between the parameters to maximize the full workspace.

3.3 Design of the underactuation parameters

We explore intervals of stiffness constants K_i from 0.5 to 10, and transmission ratio from 0.5 to 4. For each combination of parameters, we compute the size of the feasible workspace. The maximum computed feasible workspace covered 50 % of the kinematic workspace. Results are shown in the contour plots in Fig. 5, where the color code shows in dark (blue) the bigger workspaces. For this exploration, we consider no external applied force, which means that the parameters will be chosen to better compensate the force generated by the springs. Later we will show results for different applied forces.

Figure 5 shows that for each different value of transmission ratio, only the slope of the linear relationship between the stiffness constants changes. In Fig. 6 we plot the same set of data, showing the correspondence between the ratio K_3/K_2 , the transmission ratio and the obtained size of the feasible workspace. We can see that the ratio K_3/K_2 can be substantially reduced from 20 to 5 without substantially decreasing the size of the workspace. We explore this in detail next.

The parameters that resulted in the biggest workspace are

$$K_2 = 0.5, K_3 = 9.9, r = 0.9,$$

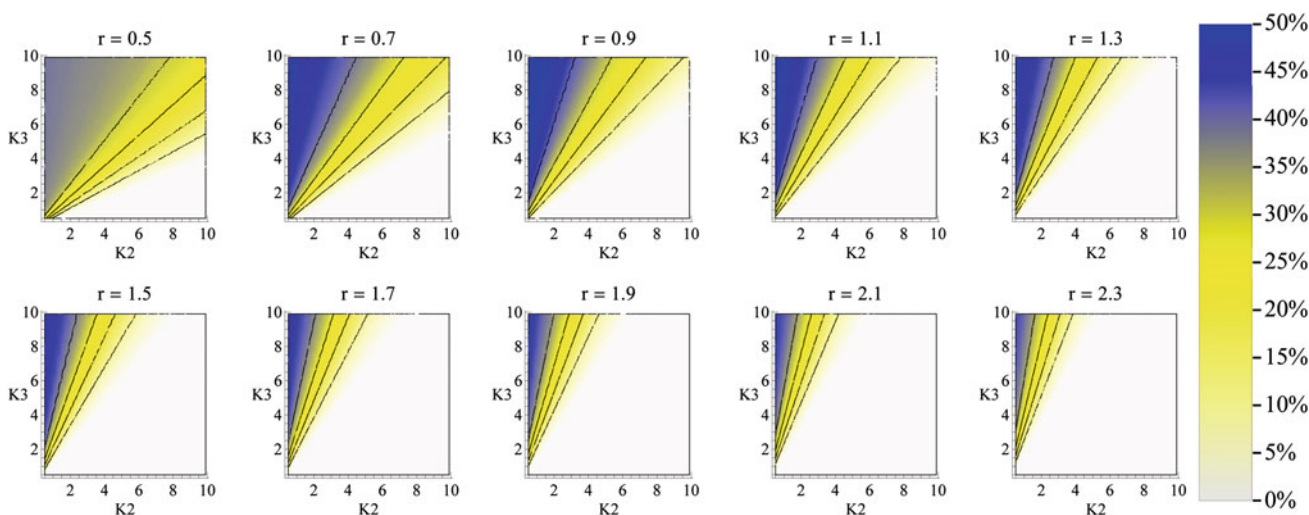


Fig. 5 Exploration of the spring stiffness constants for different values of the transmission ratio. The maximum feasible workspace spans 50 % of the kinematic workspace configurations. Darker color represents bigger feasible workspaces

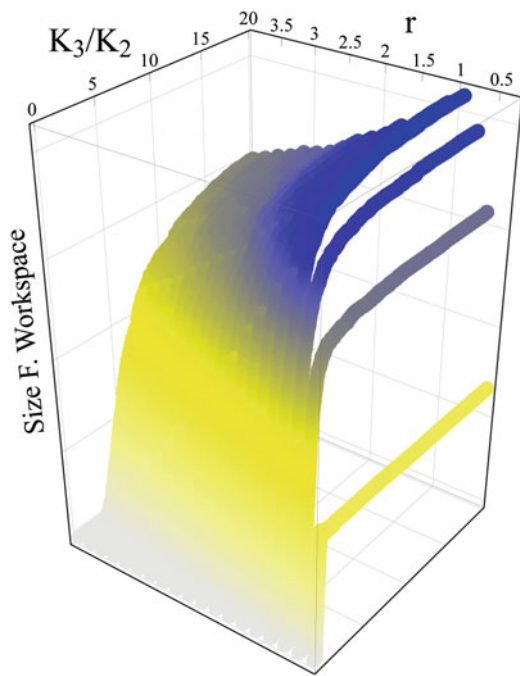


Fig. 6 Relationship between the ratio of spring stiffness constants, the transmission ratio, and the size of the feasible workspace, where the darker color represents bigger feasible workspaces following the same bar color as in Fig. 5

corresponding to a ratio $K_3/K_2 = 19.8$. In Fig. 7 (top), plot 1 shows a representation of the feasible workspace using the above parameters, where darker blue represents that more orientations can be reached from that position. Plot number 2 shows the same workspace when the applied vertical external force changes from 1 to 10 N.

In Fig. 7 (bottom) we show different histograms that correspond to the distribution of the maximum exerted motor torque per configuration. In other words, for each configuration, we compute the maximum joint torque exerted by the motors to compensate the given external force. For the histogram corresponding to the plot number 1 (in red), the bar located over 20 shows that 7% of the configurations of the feasible workspace reach a maximum motor torque of 20 Nm. Results are similar for the workspace in plot number 2, where the exerted force changes its magnitude from 1 to 10 N.

As we said before, from Fig. 6 we can observe that the stiffness ratio can be reduced to 5 or even lower without affecting at the size of the workspace. To explore this, plots 3 and 4 show the feasible workspaces for a stiffness constant ratio reduced to $K_3/K_2 = 5$, plot 3 for an exerted force of 1 N and plot 4 of 10 N. The corresponding histograms of maximum exerted torques (in purple and green) show that

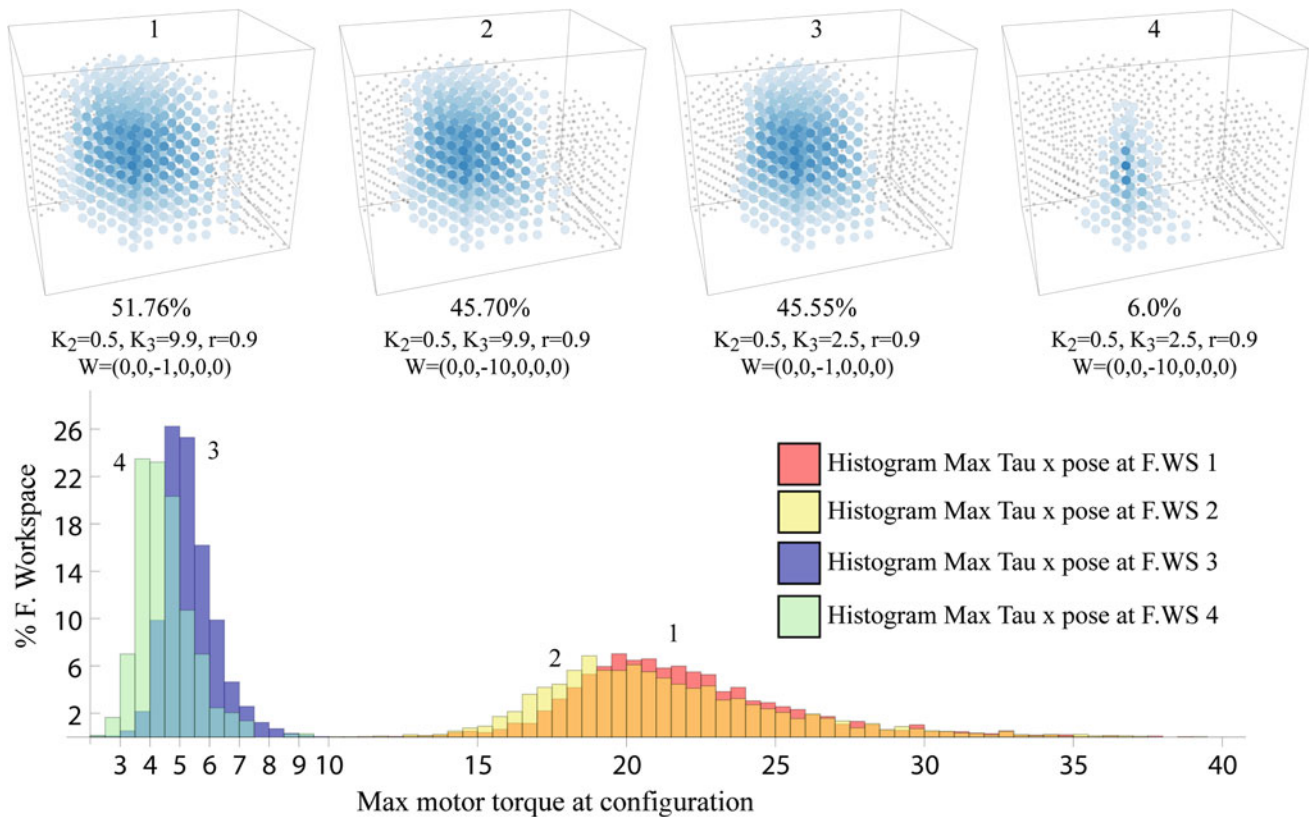


Fig. 7 Top Representation of the feasible workspace for the parameters with biggest workspaces, with different external applied forces. Bottom Four histograms of the maximum actuation torque exerted in each con-

figuration corresponding to each one of the feasible workspaces plotted above (Color figure online)

the actuation torques are substantially reduced. Therefore, reducing the stiffness ratio leads to smaller actuation torques, but at the same time, we lose robustness to external forces, because the plot number 4 shows a much reduced workspace when the external force increases to 10 N.

3.4 Discussion

The results of the parameter exploration have two clear conclusions. First, the size of the feasible workspace can be widely increased with an appropriate design of the transmission ratio and the stiffness constant ratios, but it is mainly influenced by the transmission ratio. The maximum size is obtained for a transmission ratio slightly below 1. This value may change if only a slice of the workspace is considered, as shown in [Borràs and Dollar \(2013b\)](#).

Secondly, [Fig. 6](#) shows how the ratio between the stiffness constants drastically reduces the size of the feasible workspaces when is lower than 5. However, it is fairly constant between 5 and 20. [Figure 7](#) shows how this ratio greatly changes the magnitude of the torques exerted by the motors.

Finally, in [Fig. 7](#) we can observe how the set of histograms corresponding to the same parameters and changing only the magnitude of the applied force are fairly similar. This shows that for vertical applied forces, the magnitude of the force can be increased without greatly changing the magnitude of the exerted motor torques. This is because the springs act in parallel with the motors to reduce the actuation torque. This was studied in the context of parallel manipulators in [Borràs and Dollar \(2012\)](#), showing that the actuation torque is reduced for about half of the possible directions of external applied forces.

With the presented framework, this analysis can be done for any hand using the hard-finger contact model. For example, a similar architecture with three links per finger would have the matrices \mathbf{J}_p and \mathbf{J}_Θ in [Eq. \(7\)](#) of dimensions 9×6 and 9×12 respectively, leading to a 6×12 \mathbf{J}^T in [Eq. \(9\)](#). In this case, the matrix \mathbf{J}_Θ cannot be diagonal, but is almost diagonal. Underactuation can still reduce the active Jacobian matrix \mathbf{J}_a^T in [Eq. \(12\)](#) to a 6×6 square matrix. Of course, this case is more complex because the manipulator has kinematic redundancy and thus, in each configuration the solution of the inverse kinematic has one dimension. The analysis in detail of this architecture is left as future work.

4 Conclusions

While the presented mathematical framework is not new in the context of parallel manipulators, it has not been fully explored for multifingered grasping. Robotic hands can benefit from this geometry oriented approach with applications to optimal design and singularity detection, among others.

For instance, singularities have been widely studied in the context of parallel manipulators, clearly stating the difference between fingers singularities and what are called parallel singularities, that arise from the cooperation of the fingers ([Zlatanov 1998](#)). In the context of fully actuated hands this second type of singularity occurs only in a small sub-manifold of the task space. However, the Jacobian matrix of underactuated hands can be square, and thus, the singularities of this matrix can greatly influence the size of the resultant workspace. A future study in detail of the workspace singularities can be useful for a smart hand design.

The presented framework can also model underactuated hands implemented with pulling cables. This type of hands has become very popular, but work needs to be done to understand its limitations and advantages. We have shown how underactuated hands are the equivalent of non-redundant parallel robots, making them a promising direction for dexterous manipulators, suitable both for grasping and for more easily controllable manipulation. Despite their manipulation workspace being smaller than the typical fully actuated hands, the present work shows the first steps to develop tools to design them with optimized workspaces for each task.

Acknowledgments This work was supported in part by the National Science Foundation, grant IIS-0952856.

References

- Balasubramanian, R., Belter, J. T., & Dollar, A. M. (2012). Disturbance response of two-link underactuated serial-link chains. *Journal of Mechanisms and Robotics*, *4*(2), 021013.
- Bicchi, A., Melchiorri, C., & Balluchi, D. (1995). On the mobility and manipulability of general multiple limb robots. *IEEE Transactions on Robotics and Automation*, *11*(2), 215–228.
- Birglen, L., Laliberte, T., & Gosselin, C. (2008). *Underactuated Robotic Hands*. New York: Springer.
- Borràs, J., & Dollar, A. M. (2012). *Static analysis of parallel robots with compliant joints for in-hand manipulation*. Proceedings of the IEEE/RSJ International Conference on Intelligent Robots and Systems, Portugal.
- Borràs, J., & Dollar, A. M. (2013a). *Framework comparison between a multifingered hand and a parallel manipulator*. Proceedings of the International Workshop on Computational Kinematics, Barcelona.
- Borràs, J., & Dollar, A. M. (2013b). *A parallel robots framework to study precision grasping and dexterous manipulation*. Proceedings of the IEEE International Conference on Robotics and Automation.
- Cui, L., & Dai, J. S. (2012). Reciprocity-based singular value decomposition for inverse kinematic analysis of the metamorphic multifingered hand. *Journal of Mechanisms and Robotics*, *4*(3), 034502.
- Dai, J. S., & Jones, J. R. (2001). Interrelationship between screw systems and corresponding reciprocal systems and applications. *Mechanism and Machine Theory*, *36*(5), 633–651.
- Dai, J. S., Wang, D., & Cui, L. (2009). Orientation and workspace analysis of the multifingered metamorphic hand–metahand. *IEEE Transactions on Robotics*, *25*(4), 942–947.
- Dasgupta, B., & Mruthyunjaya, T. S. (1998). Force redundancy in parallel manipulators: Theory and practical issues. *Mechanism and Machine Theory*, *33*(6), 727–742.

- Denavit, J., & Hartenberg, R. S. (1955). A kinematic notation for lower-pair mechanisms based on matrices. *ASME Journal of Applied Mechanics*, 23, 215–221.
- Dollar, A. M., & Howe, R. D. (2010). The highly adaptive SDM hand: Design and performance evaluation. *The International Journal of Robotics Research*, 29(5), 585–597.
- Downing, D., Samuel, A., & Hunt, K. (2002). Identification of the special configurations of the octahedral manipulator using the pure condition. *The International Journal of Robotics Research*, 21(2), 147–159.
- Ebert-Uphoff, I., & Voglewede, P. A. (2004). *On the connections between cable-driven robots, parallel manipulators and grasping*. Proceedings of the IEEE International Conference on Robotics and Automation, New Orleans: Parallel Manipulators and Grasping.
- Gibson, C. G., & Hunt, K. H. (1990). Geometry of screw systems—2: Classification of screw systems. *Mechanism and Machine Theory*, 25(1), 11–27.
- Gosselin, C., & Angeles, J. (1990). Singularity analysis of closed-loop kinematic chains. *IEEE Transactions on Robotics and Automation*, 6(3), 281–290.
- Hirose, S., & Umeteni, Y. (1978). The development of Soft Gripper for the Versatile Robot Hand. *Mechanism and Machine Theory*, 13, 351–359.
- Hubert, J., & Merlet, J. P. (2004). *Singularity analysis through static analysis*. Paper presented at the advances in robot kinematics.
- Hubert, J., & Merlet, J. P. (2009). Static of parallel manipulators and closeness to singularity. *Journal of Mechanisms and Robotics*, 1(1), 011011.
- Hunt, K. H., Samuel, A. E., & McAre, P. R. (1991). Special configurations of multi-finger multi-freedom grippers—A kinematic study. *The International Journal of Robotics Research*, 10(2), 123–134.
- Kanaan, D., Wenger, W., Caro, S., & Chablat, D. (2009). Singularity analysis of lower mobility parallel manipulators using Grassmann-Cayley algebra. *IEEE Transactions on Robotics*, 25(5), 995–1004.
- Kerr, J., & Roth, B. (1986). Analysis of multifingered hands. *The International Journal of Robotics Research*, 4(3), 3–17.
- Mason, M. T., & Salisbury, J. K. (1985). *Robot Hands and the Mechanics of Manipulation*. Cambridge, MA: The MIT Press.
- Merlet, J. P. (2006a). Jacobian, manipulability, condition number, and accuracy of parallel robots. *Journal of Mechanical Design*, 128(1), 199–206.
- Merlet, J. P. (2006b). *Parallel robots* (2nd ed.). New York: Springer.
- Mohamed, M. G., & Duffy, J. (1985). A direct determination of the instantaneous kinematics of fully parallel robot manipulators. *Journal of Mechanisms Transmissions and Automation in Design*, 107, 226–229.
- Mohamed, M. G., & Gosselin, C. M. (2005). Design and analysis of kinematically redundant parallel manipulators with configurable platforms. *IEEE Transactions on Robotics*, 21(3), 277–287.
- Montana, D. J. (1995). The kinematics of multi-fingered manipulation. *IEEE Transactions on Robotics and Automation*, 11(4), 491–503.
- Müller, A. (2008). Redundant actuation of parallel manipulators. In H. Wu (Ed.), *Parallel Manipulators, towards new applications*. Vienna: I-Tech Education and Publishing.
- Murray, R. M., Li, Z., & Sastry, S. S. (1994). *A mathematical introduction to robotic manipulation*. Boca Raton: CRC Press.
- Prattichizzo, D., & Trinkle, J. C. (2008). Grasping. In B. Siciliano & O. Khatib (Eds.), *Springer handbook of robotics* (pp. 671–700). Berlin: Springer.
- Romdhane, L., & Duffy, J. (1990). Kinematic analysis of multifingered hands. *The International Journal of Robotics Research*, 9(6), 3–18.
- Salisbury, J. K., & Craig, J. J. (1982). Articulated hands: force control and kinematic issues. *The International Journal of Robotics Research*, 1(1), 4–17.
- Shimoga, K. B. (1996). Robot grasp synthesis algorithms: A survey. *The International Journal of Robotics Research*, 15(3), 230–266.
- Smit, G., & Plettenburg, D. H. (2010). Efficiency of voluntary closing hand and hook prostheses. *Prosthetics and Orthotics International*, 34(4), 411–427.
- Townsend, W. (2000). The BarrettHand grasper—Programmably flexible part handling and assembly. *Industrial Robot: An International Journal*, 27, 181–188.
- Tsai, L.-W. (1999). *Robot Analysis. The mechanics of serial and parallel manipulators*. New York: Wiley.
- Zhao, J., Li, B., Yang, X., & Yu, H. (2009). Geometrical method to determine the reciprocal screws and applications to parallel manipulators. *Robotica*, 27(06), 929.
- Zlatanov, D. (1998). *Generalized singularity analysis of mechanisms*. Toronto: University of Toronto.



Júlia Borràs (M'11) received the M.Sc. degrees in mathematics and computer science from the Technical University of Catalonia, Barcelona, Spain, in 2004 and the Open University of Catalonia, Barcelona, in 2006, respectively. She received the Ph.D. degree in advanced automation and robotics from the Technical University of Catalonia, and the Spanish Scientific Research Council, Institut de Robòtica i Informàtica Industrial, Barcelona, in 2011. From 2004 to 2007, she worked with several companies as a programmer. In 2007, she joined the Institut de Robòtica i Informàtica Industrial, where she completed her Ph.D. degree. Since November 2011, she has been a Postdoctoral Associate at the Grasping and Manipulation, Rehabilitation Robotics and Biomechanics (GRAB) Laboratory, Yale University, New Haven, CT, USA.



Aaron M. Dollar is the John J. Lee Assistant Professor of Mechanical Engineering and Materials Science at Yale. He earned a B.S. in Mechanical Engineering at the University of Massachusetts at Amherst, S.M. and Ph.D. degrees in Engineering Sciences at Harvard, and conducted two years of Postdoctoral research at the MIT Media Lab. Professor Dollar's research topics include human and robotic grasping and dexterous manipulation, mechanisms and machine design, and assistive and rehabilitation devices including upper-limb prosthetics and lower-limb orthoses. He is the recipient of the 2013 DARPA Young Faculty Award, 2011 AFOSR Young Investigator Award, the 2010 Technology Review TR35 Young Innovator Award, and the 2010 NSF CAREER Award.